Supporting Information

Wang et al. 10.1073/pnas.1117790110

SI Text

Ground-Based Hydroxy Radical Data Interpolation and Error Analysis

The Fourier Transform UV-visible Spectrometer (FTUVS) measures the total hydroxy radical (OH) column from sunrise to sunset during clear and lightly cloudy days. Because OH varies substantially during the day, we use daily maximum (max) OH to eliminate the diurnal variability. Daily max OH is estimated from the second-order polynomial fit of the diurnal variation pattern (examples are provided in Fig. S1). The uncertainty of the daily max estimate is determined by the rmsd of the measured points from the fit. After screening out bad days due to various reasons (e.g., weather conditions or instrument alignment only allows partial day measurements that are not long enough for reliable diurnal fits), there are about 750 data points. A few longer gaps of more than 1 mo are due to measurement campaigns for other species or instrument upgrades. The screened daily max and the corresponding uncertainty are plotted in Fig. S2*A*.

To perform fast Fourier transform (FFT) analysis, the gaps in the time series need to be filled by interpolation. To reduce the uncertainty due to the day-to-day variability (may originate from reasons that include the tropospheric OH variability due to chemical reactions irrelevant for this study, the middle atmospheric OH variability due to short-term solar UV changes, and instrument noise), we first calculated monthly means for the months with available OH data (black circles in Fig. S2*B*). Note that the mean date of the monthly mean calculation may not be the middle of the month, depending on the available dates with OH data. We then use linear interpolation to derive an estimate of the daily max OH for each day (black lines in Fig. S2*B*). To validate this interpolation, we also applied the missing data filling using kSpectra Toolkit software (www.spectraworks.com/), which is specialized in finding small signals through advanced spectral analysis of multivariate time series based on the mathematical methods described by Ghil et al. (1). The results are very similar to the linear interpolation. The estimated uncertainty (χ^2 analysis) of the interpolated data is about 4×10^{12} cm^{-2}. We adopt this uncertainty as the error bar of all our interpolated daily OH max values (light gray shade in Fig. S2*C*), although the actual uncertainty of the monthly mean points in Fig. S2*B* is smaller.

The FFT smoothing analysis is carried out using the interpolated daily max OH. To avoid an "edge effect" of the trend analysis, particularly for a signal with a period that is close to the length of the time series, we extended the OH data (using data in the adjacent year) at the beginning and the end of the time series to the closest date when the OH value is similar to the annual mean of the corresponding year. The extended time series is shown in blue in Fig. S2*C*. After the FFT analysis (dashed green and red lines in Fig. S2*C*), we truncate the results to exclude the extensions (solid green and red lines in Fig. S2*C*).

To evaluate the impact of the uncertainties (within 4×10^{12} cm^{-2}) of the interpolated data on our FFT results, we applied a Monte Carlo analysis (2). The daily max OH data in Fig. S2*C* are allowed to vary randomly and independently within the error bar range to construct a new dataset for FFT analysis. Such calculations are repeated 1,000 times. The resulting 2-y FFT analysis result that represents the OH SC signal varies around the 10% value (peak-to-valley change in OH) by ±0.5%. Thus, the impact of the uncertainty in missing data filling on our analysis is found to be small.

We also applied an independent regression analysis to derive the SC signal. The long-term Lyman-α index was used as a proxy. The results are found to be similar to FFT results. During the regression analysis, an index describing the vertical propagation of the quasibiennial oscillation in the stratosphere was also considered and found to be insignificant. The effect of El Niño/La Niña-Southern Oscillation was also found to be negligible.

Solar Spectral Irradiance Variability and the Related Debates

The Solar Radiation and Climate Experiment (SORCE) solar spectral irradiance (SSI) variability used in our modeling study is constructed using SSI data from the SORCE/Solar Stellar Irradiance Comparison Experiment (SOLSTICE) and SORCE/spectral irradiance monitor (SIM), with the combination cutoff at a wavelength of 210 nm or 240 nm (in two sets of model runs, as described in the main text). The SOLSTICE makes daily UV SSI measurements and compares them with the irradiance from an ensemble of 18 stable early-type stars. This approach provides accurate monitoring and calibration of instrument in-flight performance (3). The absolute accuracy for the wavelength region used in our study is mostly within 3%. The uncertainty of the corresponding SSI trend analysis is within 2%. SIM SSI measurements have been made with two independent spectrometer channels with an accuracy of better than 2% (4). Based on the comparison of data from the two channels, the long-term trend uncertainty is estimated to be within ∼0.5%, ∼0.2%, and ∼0.05% in the wavelength regions of 200–300 nm, 300–400 nm, and 400–1600 nm, respectively. The methods of performing instrument degradation corrections based on a two-channel comparison and then extracting long-term SSI variability are described in the auxiliary materials of a study by Harder et al. (5), and they are very similar to the methods used for the SORCE/total irradiance monitor instrument [for total solar irradiance (TSI) measurements; data shown in Fig. 2]. Although the degradation of the instruments in recent years (mostly since 2009) is a known issue and the corresponding data correction and calibration have been an ongoing work during their future version development (http://lasp.colorado.edu/sorce/data/ssi_data.htm), the SSI variability used in our study is taken from measurements during 2004–2007 (6) when instruments had the most reliable performance, and the data thus have the best quality.

To estimate the SSI variability from solar max to solar minimum (min), we use a scaling factor to extend the SSI variability from May 2004–November 2007 back to January 2002 (about the max of SC 23), assuming that SSI in November 2007 is reasonably close to that of the solar min (2008–2009):

$$f(\lambda) = \frac{S_{\odot,\lambda}(\text{Jan } 2002) - S_{\odot,\lambda}(\text{Nov } 2007)}{S_{\odot,\lambda}(\text{May } 2004) - S_{\odot,\lambda}(\text{Nov } 2007)},$$

where $S_{\odot,\lambda}$ is the solar irradiance at wavelength λ.

The scaling factor $f(\lambda)$ is estimated using the Mg-II index variability as a proxy. The results are shown in Fig. 4 (*Inset*).

Similar combined SORCE SSI variability has been used in a number of modeling studies (e.g., refs. 7–9) following the first such study by Haigh et al. (6) in 2010. The decrease in SORCE SSI (especially SIM data) during 2004–2007 suggests "a four to six times larger decline in ultraviolet than would have been predicted on the basis of our previous understanding. This reduction was partially compensated in the total solar output by an increase in radiation at visible wave-lengths" (6). The previously

well-accepted SSI variability is from the Naval Research Laboratory (NRL) model based on observations of solar parameters during previous solar cycles (SCs) (10, 11), in which F10.7 serves as a primary proxy for the SC. The corresponding UV variability is characterized by the fractional changes from solar max to solar min, assuming that the spectral variability follows the phase of F10.7. The NRL model also requires other solar quantities, including the sunspot number and the daily planetary K and a indices.

The unexplainable large discrepancies between SORCE SSI and the well-known NRL SSI have sparked investigations from various perspectives and a continuing debate since 2011. For example, Fontenla et al. (12) developed an improved solar physics model (considering more solar parameters during both "active" and "quiet" periods of the Sun to describe the SSI variability; more comprehensive than the NRL model) and generated results that agree better with SORCE SSI. Studies on atmospheric SC signal in ozone by Merkel et al. (7) show a comparison of satellite observations with model simulations and suggest that SORCE solar forcing appears to explain the observations better. In contrast, an updated study from the NRL team concluded that "the SORCE SIM observations should be used with extreme caution in studies of climate and atmospheric change until additional validation and uncertainty estimates are available" (13). Moreover, DeLand and Cebula (14) believe "the most likely explanation for these results (i.e., SORCE SSI decreases much faster than previous believed) is an incomplete characterization of SORCE on-orbit instrument degradation effects." This conclusion was primarily based on comprehensive comparisons between SORCE SSI variability and observations from previous SCs, assuming that SSI variability during SC 23 has similar behavior to that during previous SCs. However, the investigations of Lukianova and Mursula (15) showed the "changed relation between sunspot numbers, solar UV/EUV radiation, and TSI during the declining phase of SC 23," suggesting that the declining phase of SC 23 might be substantially different from those of previous SCs. The SSI debates are still continuing, and there will be more studies and publications on the way.

There is no doubt that there are many questions to be answered, and further research and discussions from various perspectives are required before a consensus on this issue can be established in the scientific community. Our study of OH response to the SC contributes to the continuing discussions by providing unique and independent evidence from the point of view of the Earth's atmosphere and by conducting important sensitivity assessments of the role of solar forcing uncertainty in atmospheric OH variabilities.

1. Ghil M, et al. (2000) Advanced spectral methods for climatic time series. *Rev Geophys* 40(1):3.1–3.41, 10.1029/2000GR000092.
2. Bevington PR, Robinson DK (2002) *Data Reduction and Error Analysis for the Physical Sciences* (McGraw–Hill, New York), 3rd Ed.
3. Snow M, et al. (2005) Solar-Stellar Irradiance Comparison Experiment II (SOLSTICE II): Examination of the solar-stellar comparison technique. *Sol Phys* 230:295–324.
4. Harder JW, et al. (2010) The SORCE SIM solar spectrum: Comparison with recent observations. *Sol Phys* 263:3–24.
5. Harder JW, Fontenla JM, Pilewskie P, Richard EC, Woods TN (2009) Trends in solar spectral irradiance variability in the visible and infrared. *Geophys Res Lett* 36:L07801.
6. Haigh JD, Winning AR, Toumi R, Harder JW (2010) An influence of solar spectral variations on radiative forcing of climate. *Nature* 467(7316):696–699.
7. Merkel AW, et al. (2011) The impact of solar spectral irradiance variability on middle atmospheric ozone. *Geophys Res Lett* 38:L13802.
8. Swartz WH, et al. (2012) Middle atmosphere response to different descriptions of the 11-yr solar cycle in spectral irradiance in a chemistry-climate model. *Atmos Chem Phys* 12:5937–5948, 10.5194/acp-12-5937-2012.
9. Li K-F, et al. (2012) Simulation of solar-cycle response in tropical total column ozone using SORCE irradiance. *Atmospheric Chemistry and Physics Discussions* 12:1867–1893.
10. Lean JL, et al. (1997) Detection and parameterization of variations in solar mid- and near-ultraviolet radiation (200-400 nm). *J Geophys Res Atmos* 102:29939–29956.
11. Lean J (2000) Evolution of the sun's spectral irradiance since the Maunder Minimum. *Geophys Res Lett* 27(16):2425–2428.
12. Fontenla JM, et al. (2011) High-resolution solar spectral irradiance from extreme ultraviolet to far infrared. *J Geophys Res* 116:D20108.
13. Lean JL, DeLand MT (2012) How does the Sun's spectrum vary? *J Clim* 25:2555–2560.
14. DeLand MT, Cebula RP (2012) Solar UV variations during the decline of Cycle 23. *J Atmos Sol Terr Phys* 77:225–234.
15. Lukianova R, Mursula K (2011) Changed relation between sunspot numbers, solar UV/EUV radiation and TSI during the declining phase of solar cycle 23. *J Atmos Sol Terr Phys* 73:235–240.

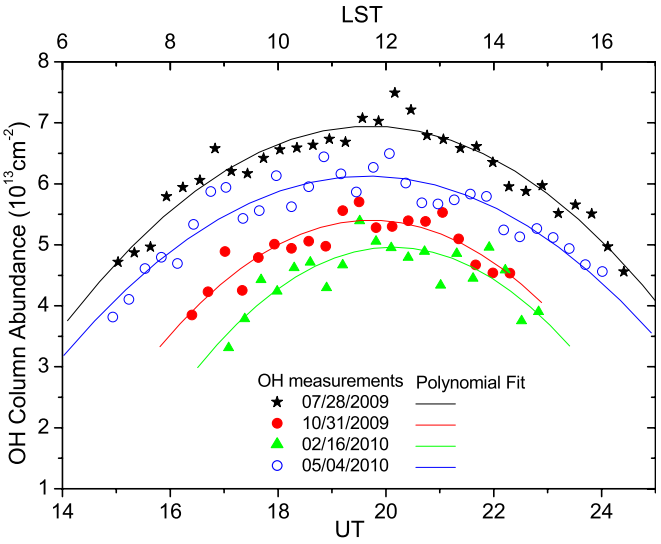

Fig. S1. Examples of the diurnal variability of Fourier transform UV-visible spectrometer (FTUVS) OH data at the Table Mountain Facility (TMF) during four seasons. The selected dates are 07/28/2009 (black), 10/31/2009 (red), 02/16/2010 (green), and 05/04/2010 (blue). The scatters show the measured data. The lines are the polynomial fit of the diurnal variation during each day. This polynomial fit is used to determine the daily max OH abundance at the TMF.

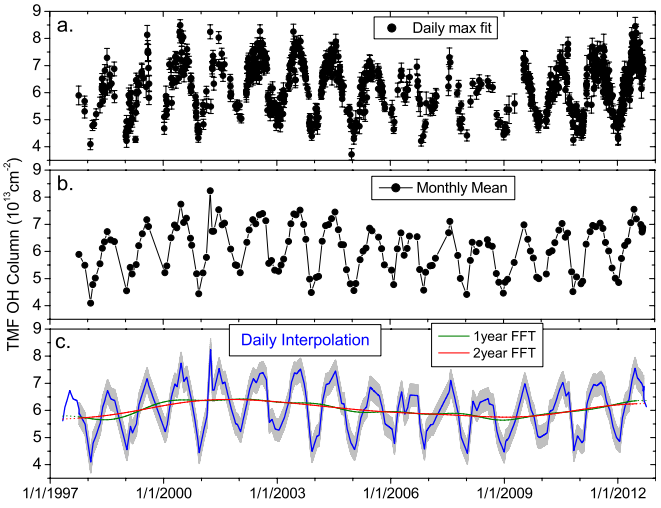

Fig. S2. Time series of daily max Fourier transform UV-visible spectrometer (FTUVS) OH data and the interpolation of missing data. (*A*) Daily max OH determined by the polynomial fit of the diurnal pattern of each day (Fig. S1). Error bars represent the rms uncertainty of the polynomial fit. (*B*) Monthly mean of daily max OH. (*C*) Monthly mean data in *B* are linearly interpolated into daily data (blue line) for FFT analysis (red and green lines). The error is estimated using the Kspectra software.

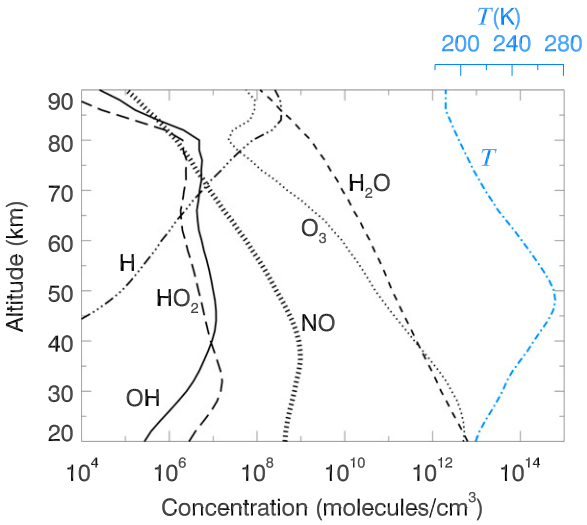

Fig. S3. Simulated diurnally averaged OH and other species related to odd-hydrogen (HO_x) chemistry and the adopted temperature in the 1D model. *T*(K) represents temperature in Kelvin and uses a separate horizontal scale (in blue).

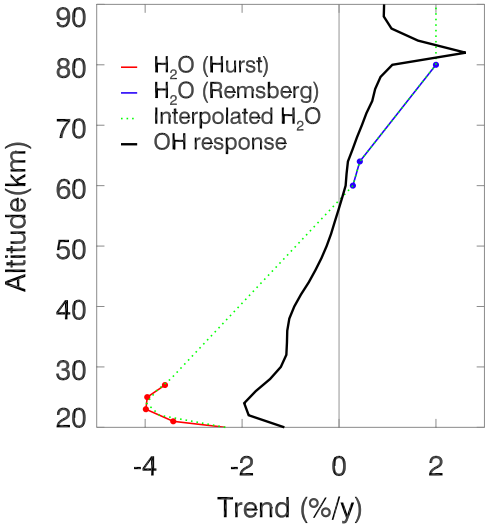

Fig. S4. Trend in H_2O and the corresponding OH change from 1D model simulations. The color line shows the trend in H_2O based on the stratospheric trend during 2000–2005 reported by Hurst et al. (1), the mesospheric trend reported by Remsberg (2), and linear interpolation for other altitudes. The black line shows the 1D model result of OH change in response to the H_2O trend. Note that Remsberg (2) also reported an SC-like decadal variability in mesospheric H_2O, which we do not consider as a long-term trend to avoid accounting for the SC response twice. Our 1D model can nicely simulate such an SC-like decadal variability in mesospheric H_2O.

1. Hurst DF, et al. (2011) Stratospheric water vapor trends over Boulder, Colorado: Analysis of the 30-year Boulder record. *J Geophys Res Atmos* 116:D02306.
2. Remsberg E (2010) Observed seasonal to decadal scale responses in mesospheric water vapor. *J Geophys Res Atmos* 115:D06306.

Other Supporting Information Files

Dataset S1 (TXT)